Bull. Chem. Soc. Jpn., 70, 1777—1785 (1997)

Theoretical Explanation of the Hydrogen Wave on a Platinum Single Crystal Electrode

Hideyuki Narumi

Division of Material Science, Graduate School of Environmental Earth Science, Hokkaido University, Kita-ku, Sapporo 060

(Received February 6, 1997)

Voltammograms observed on basal planes of a Pt single crystal electrode in 0.1 M $HClO_4$ were analyzed theoretically. Adsorbed hydrogen atoms were assumed to form 2-dimensional (111), (100), and (110) lattices. These lattices were treated by applying the Hückel method to an elementary domain consisting of 400×200 lattice points with periodic boundary conditions. Results explained the essential aspects of the butterfly at Pt(111) and the hydrogen waves at Pt(100) and Pt-(110). The lateral interactions of the adsorbed hydrogen atoms were attractive in all cases and their values were estimated. The value at Pt(110) reproduced the previous one derived from the adsorption isotherm analysis. The square-shaped wave observed at Pt(111) in a potential range of 0.05—0.35 V was explained by an entirely different model for a freely moving particle. The analysis suggested that the square wave is due to electrons which move freely in the adsorption layer. The Hückel method was further applied to 3-dimensional lattices having 2 to 3 layers. Results suggested a striking effect of the absorbed hydrogen beneath the surface on the hydrogen wave.

The hydrogen wave on platinum electrode has been extensively studied. Recently Pt single crystals became easily available in the laboratory by the melt and quench method[1] and studies have produced many useful data in electrochemistry. The electrochemical approach has a great advantage in that it can follow a trace amount of chemical change on the single crystal surface precisely, even an amount of submonolayer on a tiny surface of say 0.1 cm^2. Interestingly, the single crystal in an electrochemical system has been proved to resist contaminations for a sufficient time, though it is immersed in a condensed system in contrast to UHV system.

It is now well known that the hydrogen waves on Pt single crystal electrodes differ sensitively by the structure of the surface, as already reviewed.[2] The characteristic aspects of each hydrogen wave observed on basal planes are described later (Section 1). To be mentioned here is that Pt(111) plane reveals an additional wave of square pattern in a potential range of 0.05—0.35 V. This square wave is analyzed separately on an entirely different model in Section 3.

The main aim of the present study is to explain the hydrogen waves observed on Pt(111), Pt(100), and Pt(110) in $HClO_4$ solution by the Hückel approximation with boundary conditions[3,4] as one of the chemical applications of the graph theory (Section 2).[5—13]

Only a few works have been reported on the theoretical analysis of the hydrogen wave by taking into account the lateral interaction of the adsorbates, which depends on their arrangement on the surface.

A precise statistic-mechanical treatment of the interaction has been first conducted in relation to the hydrogen electrode reaction on Ni(111), Ni(100), and Ni(110) surfaces.[14,15] Adsorption isotherms and the reaction rates calculated in terms of partition functions revealed remarkable structure dependences. This treatment was applied later to the hydrogen adsorption isotherm on Pt(111), Pt(100), and Pt(110) surfaces; it reproduced the hydrogen wave on Pt (poly crystal) under the assumption of an equal exposure of the basal planes.[16] These works were conducted before the single crystal electrode became available. It should be remembered that repulsive interactions were assumed in the calculations.

Lately, a statistical mechanical treatment of redox couples and an activated complex confined to electrode surfaces at monolayer levels have been reported, in which interaction energies and molecular arrangements are taken into account by using a two-dimensional quasi-crystalline lattice model.[17] A general expression of the current–potential relationship is derived for one-step surface redox-electrode reactions of the above species based on the transition-state rate theory.

The expression was then applied to reversible and irreversible cyclic voltammograms as functions of the interaction parameters, kinetic parameters, and coordination number.[18] Furthermore, equations for the faradaic impedance were also treated.[18]

In the present study, the Hückel method is used where the interaction is introduced by the graph theory. 'An elementary domain' consisting of a limited number of platinum atoms acts as an unit of the plane and the boundary end effect of the domain was eliminated by introducing a periodic condition at the boundary. This procedure will allow one to calculate the eigenvalues for an infinite surface by using the elementary domain.[19,20]

The present calculations completely differ from the statistic-mechanical treatments. All the adsorbates are treated as one macromolecule as a whole. It is interesting to see that

this simple macromolecule treatment by the Hückel approximation with boundary conditions can reproduce the sharp characteristic peaks of the hydrogen waves on Pt(111), Pt-(100), and Pt(110). The attractive interaction turned out to be effective.

On the other hand, the square wave on Pt(111) has received nontheoretical treatments. Treatments in terms of adsorption isotherm can not, in principle, explain the square shape of the wave even if various repulsive interactions are introduced, since they all give more or less a bell-shaped wave. The explanation must be given on an entirely different model. The present study shows that the free particle model[21] is effective for explaining the phenomenon. This means that when a coverage exceeds 1/3, the adsorption state of hydrogen atom changes completely. This explanation gives quite a new insight into the study of adsorbed hydrogen atoms on the Pt(111) surface.

Empirical features of the hydrogen wave are first summarized below. Analyzed results are further discussed in Section 4.

1. Characteristic Aspects of the Hydrogen Wave

Typical hydrogen waves observed on Pt(111), Pt(100), and Pt(110) in 0.1 M $HClO_4$ (1 M = 1 mol dm^{-3}) are represented in Figs. 1 and 2 by dotted lines. The waves are highly sensitive to the surface structure as well as to the kind of anion.

1-1. Pt(111). A square wave appears in a potential range of 0.05—0.35 V independent of the anions. To the more positive side appears an unsymmetric wave with a peak in both solutions. In $HClO_4$, the wave locates in a potential range of 0.6—0.9 V and is called a 'butterfly' after its shape. The peak potential is 0.79 V. In H_2SO_4, a wave corresponding to the butterfly appears in a much more negative range of 0.32—0.50 V with a sharp peak at 0.45 V. The butterfly in $HClO_4$ shifts markedly in the negative direction by addition of extremely small amounts of H_2SO_4 (ca. 10^{-5} M)[22] and H_3PO_4 (ca. 10^{-4} M).[23] Such a shift has been attributed to a specific adsorption of the respective anions.

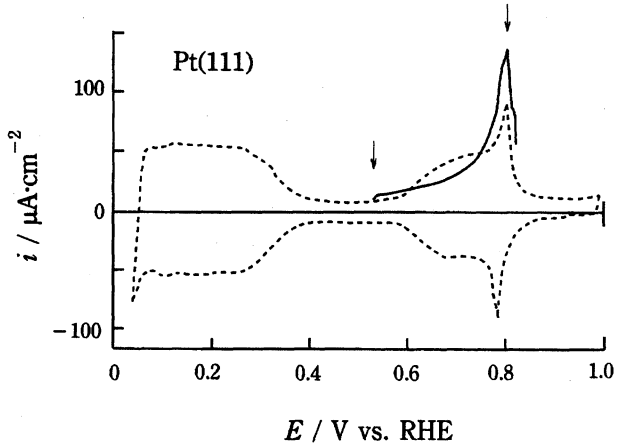

Fig. 1. Hydrogen waves (dotted line: 0.1 M $HClO_4$, sweep rate 50 mV s^{-1}) and density of state (solid line, $M \times N$ = 400×200) on Pt (111).

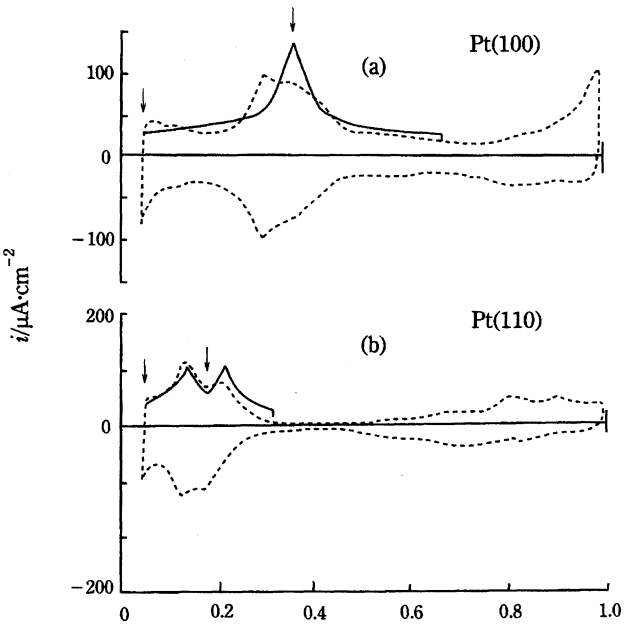

Fig. 2. Hydrogen waves (dotted line; 0.1 M $HClO_4$, sweep rate 50 mV s^{-1}) and density of state (solid line, $M \times N$ = 400×200) on a) Pt(100) and b) Pt(110).

1-2. Pt(100). The hydrogen wave is entirely different from that on Pt(111), reflecting a structure-sensitiveness. In $HClO_4$, the wave observed at a positive-going scan reveals double peaks which become much clearer in H_2SO_4. Interestingly, the locations of two peaks are not so much affected by changing the solution to H_2SO_4. Detailed studies[24,25] in H_2SO_4 show that a well oriented surface grows the positive side peak and depresses the negative one. Thus the positive side peak will be taken to reflect the intrinsic aspect of Pt(100).

A negative-going scan gives an entirely different wave with a predominating peak at almost the same potential of the negative side peak. Such a change will be closely related to the surface reorientation caused by the potential scan to 1.0 V.

1-3. Pt(110). The hydrogen wave appears in the most negative potential range of 0.05—0.30 V in both solutions. Hydrogen atoms adsorb most weakly on Pt(110). In $HClO_4$, the hydrogen wave appears again with double peaks. To the contrary, in H_2SO_4 it gives a well defined sharp peak at 0.13 V. We have analyzed the latter peak by a kinetic approach under the equilibrium condition of the proton discharge and the ionization of the adsorbed hydrogen atom.[26]

Hydrogen Waves Subjected to Analysis. The hydrogen waves examined were those obtained at a positive-going scan in $HClO_4$ in order to exclude possible effects of the specific adsorption of sulfate ion and the surface reorientation. In addition, we subjected the positive side peak of Pt(100) and the double peaks on Pt(110) to the following analysis. The potential range and the peak potential of each hydrogen wave

examined are listed in Table 1.

2. Analysis of Hydrogen Waves, Except for the Square Part

2.1. Model and Introduction of Lateral Interactions by Graph Theory. Adsorbed hydrogen atoms are taken to form a 2-dimensional lattice at a monolayer coverage at the initiation of the hydrogen wave, i.e., at 50 mV. The lattice has the same arrangement as that of platinum atoms on each crystal plane. Although the platinum atoms on a single crystal plain provide physically equal adsorption sites, the adsorbed hydrogen atoms can have different adsorption energies. If the adsorption energy had only one value, the formation and ionized desorption of adsorbed hydrogen atoms H(a)'s by

$$H^+ + e^- \rightleftarrows H(a) \tag{1}$$

would take place at a pinned potential and never give a wave such as that observed.

In the present study, the structure of the energy distribution is assumed as the first approximation to remain constant during the ionization of H(a) giving the hydrogen wave.

In addition, the energy distribution of H(a) will be taken to be predominant factor, and a possible contribution of H^+ energy distribution was not treated as a first approximation.

The macromolecule consisting of hydrogen atoms in 2-dimensional lattices can, in principle, have various energy levels. Their distributions can be obtained by using the graph theory (the Hückel method) of mathematical chemistry.[5—13] Boundary periodic conditions are applied to elementary domains in order to eliminate end effects.[19,20]

As stated earlier, we choose an elementary domain specified with M and N lattice points arranged in the two directions. Each lattice point is numbered as 1, 2, $\cdots$, i $\cdots$, n, where n=MN.

This system is treated basically in the same way as for π-electron systems, where π-electrons interact weakly with each other.

The total energy E of the system derived from the wave equation

$$H\Psi = E\Psi \tag{2}$$

with the total wave function

$$\Psi(1,2,\cdots,n) = \phi_1(1)\cdot\phi_2(2)\cdots\phi_n(n), \tag{3}$$

and the Hamiltonian

$$H = h(1) + h(2) + \cdots + h(n) \tag{4}$$

Table 1. Potential Range of Hydrogen Wave and Peak Potential (vs. RHE)

Plane		Potential range/V	Peak potential/V
Pt(111)	Square wave	0.05—0.35	—
	butterfly	0.54—0.9	0.79
Pt(100)		0.05—0.65	0.35
Pt(110)		0.05—0.29	0.14, 0.22

is given as

$$E = \varepsilon_1 + \varepsilon_2 + \cdots + \varepsilon_n \tag{5}$$

by solving the following type of secular equation:

$$\det \begin{bmatrix} \alpha_1-\varepsilon & \beta_{12} & \beta_{13} & \beta_{14} & \beta_{15} & \beta_{16} & \beta_{17} & 0\cdots \\ \beta_{21} & \alpha_2-\varepsilon & \beta_{23} & 0 & 0 & 0 & \beta_{27} & \cdots \\ \beta_{31} & \beta_{32} & \alpha_3-\varepsilon & \beta_{34} & 0 & 0 & 0 & \cdots \\ \beta_{41} & 0 & \beta_{43} & \alpha_4-\varepsilon & \beta_{45} & 0 & 0 & \cdots \\ \beta_{51} & 0 & 0 & \beta_{54} & \alpha_5-\varepsilon & \beta_{56} & 0 & \cdots \\ \beta_{61} & 0 & 0 & 0 & \beta_{65} & \alpha_6-\varepsilon & \beta_{67} & \cdots \\ \beta_{71} & \beta_{72} & 0 & 0 & 0 & \beta_{76} & \alpha_7-\varepsilon & \cdots \\ \cdot & \cdot & \cdot & \cdot & \cdot & \cdot & \cdot & \\ \cdot & \cdot & \cdot & \cdot & \cdot & \cdot & \cdot & \\ \cdot & \cdot & \cdot & \cdot & \cdot & \cdot & \cdot & \end{bmatrix} = 0 \quad \text{for (111)} \tag{6}$$

where α_i and $\beta_{i,j}$ have the usual meanings. The wave function $\phi_i(i)$ stands for the wave function of an electron of i-th hydrogen atom adsorbed on the lattice. The Hamiltonian $h(i)$ is a one-electron Hamiltonian for ith-electron. The above equation becomes easily soluble by a graph-theoretical method when we put

$$\alpha_1 = \alpha_2 = \alpha_3 = \cdots \equiv \alpha$$
$$\beta_{12} = \beta_{13} = \cdots = \beta_{i,j} \equiv \beta \ (i \neq j),$$

since all the non-diagonal elements of the matrix become 0 or β.

When the determinant of Eq. 6 is divided by β, the non-diagonal elements become 1 or 0.

The introduction of the interactions is explained in detail for Pt(111). A Pt(111) surface has the largest number of nearest neighboring lattice points among the three kinds of lattices. There are 6 nearest neighboring lattice points around each lattice point i of interest. The lattice point i is specified by two components of i_1 and i_2. Six neighboring lattice points, named j's are distinguished from each other with 2 directional components as follows:

$$(i_1, i_2+1),\ (i_1+1, i_2+1),\ (i_1-1, i_2),\ (i_1+1, i_2),$$
$$(i_1-1, i_2-1),\ (i_1, i_2-1)$$

An adsorbed hydrogen atom on the lattice point (i_1,i_2) interacts with six nearest hydrogen atoms. The interaction appears in the corresponding matrix elements expressed in a general form in terms of δ functions as:

$$\begin{aligned} A_{i,j} = {} & \delta(i_1,j_1-1)\cdot\delta(i_2,j_2) + \delta(i_1j_1)\cdot\delta(i_2,j_2-1) \\ & + \delta(i_1,j_1-1)\cdot\delta(i_2,j_2-1) + \delta(i_1,j_1+1)\cdot\delta(i_2,j_2) \\ & + \delta(i_1,j_1)\cdot\delta(i_2,j_2+1) + \delta(i_1,j_1+1)\cdot\delta(i_2,j_2+1), \end{aligned} \tag{7}$$

where j_1 and j_2 represent two directional components of j's and can have six sets of values stated above. $\delta(i_1,j_1)\cdot\delta(i_2,j_2)$ becomes 1 at i_1=j_1 and i_2=j_2 and 0 in other cases, depending on whether the two lattice points are bounded or not.

Matrix elements $A_{i,j}$ for the Pt(100) or Pt(110) lattices are obtained by deleting the 3rd and 6th terms.

A similar procedure has been used in a graph-theoretical application in fields of mathematical chemistry and statistical mechanics.[19,20]

2.2. Procedure of Calculation. First, the matrix element $A_{i,j}$ is diagonalized with the Fourier-type eigenvector to obtain eigenvalues.[3,4,19,20]

The Fourier-type eigenvector $Z_j^{(k_1,k_2)}$, where k_1 and k_2 stand for two components of a wave number vector k, is expressed as follows:

$$Z_j^{(k)} \equiv Z_j^{(k_1,k_2)} \equiv Z_{j_1j_2}^{(k_1,k_2)} = \exp\{(2\pi i/M)k_1j_1\} \times \exp\{(2\pi i/N)k_2j_2\} \equiv e_1(k_1j_1)e_2(k_2j_2) \quad (8)$$

where $Z_j^{(k)}$ is an abbreviation of $Z_{j_1j_2}^{(k_1,k_2)}$. Exponentials $\exp\{(2\pi i/M)k_1j_1\}$ and $\exp\{(2\pi i/N)k_2j_2\}$ are abbreviated as $e_1(k_1j_1)$ and $e_2(k_1j_2)$, respectively. A matrix element $A_{i,j}$ multiplied by the eigenvector is summed up from $j_1=1$, $j_2=1$ to $j_1=(M-1)$, $j_2=(N-1)$ in order to solve an eigenvalue problem. It must be mentioned that this summation implied $j_M=j_1$ and $j_N=j_2$. Namely, a periodic boundary condition is introduced in the two directions; such an introduction results in the elimination of the end effects. The results obtained reflect the values on the surface extending in the two directions by the repetition of the elementary domain without limit.

The summation gives the following relation:

$$\begin{aligned}
&\sum_{j}^{(M-1)(N-1)} A_{i,j}Z_j^{(k)} \\
&= \sum_{j_1j_2}\{\delta(i_1,j_1-1)\cdot\delta(i_2,j_2)+\delta(i_1,j_1)\cdot\delta(i_2,j_2-1)+\cdots\} \\
&\quad \times e_1(k_1,j_1)e_2(k_2,j_2) \\
&= e_1(k_1(i_1+1))e_2(k_2i_2)+e_1(k_1(i_1-1))e_2(k_2i_2) \\
&\quad +e_1(k_1i_1)e_2(k_2(i_2+1))+e_1(k_1i_1)e_2(k_2(i_2-1)) \\
&\quad +e_1(k_1(i_1+1))e_2(k_2(i_2+1))+e_1(k_1(i_1-1))e_2(k_2(i_2-1)) \\
&= \begin{bmatrix} e_1(k_1) & + & e_1(-k_1) \\ + & e_2(k_2) & + & e_2(-k_2) \\ + & e_1(k_1) & \times & e_2(k_2) \\ + & e_1(-k_1) & \times & e_2(-k_2) \end{bmatrix} e_1(k_1i_1)e_2(k_2i_2) \\
&= \lambda_{k_1,k_2}Z_i^{(k_1,k_2)} \equiv \lambda_{k_1,k_2}Z_i^{(k)} \quad (9)
\end{aligned}$$

Eigenvalues λ_k's are obtained from the above equation for Pt(111), Pt(100), and Pt(110) respectively as follows.

Pt(111) (Triangle Lattice).

$$\lambda_k \equiv \lambda_{k_1,k_2} = 2[\cos 2\pi k_1/M + \cos 2\pi k_2/N + \cos(2\pi k_1/M + 2\pi k_2/N)] \quad (10)$$

Pt(100) (Square Lattice) and Pt(110) (Rectangular Lattice).

$$\lambda_k = 2[\cos 2\pi k_1/M + \cos 2\pi k_2/N]. \quad (11)$$

The expression of eigenvalues for a square lattice is the same as for rectangular lattice because the eigenvalues do not contain distances between atoms.

One of the simplest examples to explain the above calculations, the case of (100), $M=N=3$, is shown as follows:

The number of the matrix elements $A_{i,j}$ is $((M-1)(N-1))^2=((3-1)(3-1))^2=16$ after the end effect is eliminated, namely the two edges are connected.

Let us give a coordinate (1, 1) to the center lattice point (denoted 1). This point is surrounded by 8 lattice points on a 3×3 lattice. But only 4 points 1(1, 1), 2(1, 2), 3(0, 2), and 4(0, 1) are treated here because 3(0, 2) is 5(0, −1), 2(1, 2) is 6(1, −1) and 9(2, 2) is 7(2, −1); at the same time, 9(2, 2) is 3(0, 2) and 8(2, 1) is 4(0, 1). The above procedure means that a torus or 'doughnut' surface is made from a 3×3 lattice. The end effect is eliminated by the above procedure.

Some of $A_{i,j}$ terms are shown as follows, according to Eq. 7 with deleting the 3rd and 6th terms:

$$\begin{aligned}
A_{1,2} &= \delta(1,1-1)\delta(1,2)+\delta(1,1)\delta(1,2-1) \\
&\quad +\delta(1,1+1)\delta(1,2)+\delta(1,1)\delta(1,2+1) = 1 \\
A_{1,3} &= \delta(1,0-1)\delta(1,2)+\delta(1,0)\delta(1,2-1) \\
&\quad +\delta(1,0+1)\delta(1,2)+\delta(1,1)\delta(1,2+1) = 0 \\
&\cdots\cdots
\end{aligned}$$

The elements of the Fourier-type eigenvector $Z_{j_1j_2}^{(k_1,k_2)}$ in Eq. 8 are shown in this case as follows:

$$\begin{aligned}
Z_1^{(k)} &= Z_{11}^{(k_1,k_2)} = \exp\{(2\pi i/2)k_1\}\exp\{(2\pi i/2)k_2\} \\
Z_2^{(k)} &= Z_{12}^{(k_1,k_2)} = \exp\{(2\pi i/2)k_1\}\exp\{(2\pi i/2)k_2\times 2\} \\
Z_3^{(k)} &= Z_{21}^{(k_1,k_2)} = \exp\{(2\pi i/2)k_1\times 2\}\exp\{(2\pi i/2)k_2\} \\
Z_4^{(k)} &= Z_{22}^{(k_1,k_2)} = \exp\{(2\pi i/2)k_1\times 2\}\exp\{(2\pi i/2)k_2\times 2\}
\end{aligned}$$

where $k_1=0$, 1 and $k_2=0$, 1.

$Z_{11}^{(11)}=1$, $Z_{12}^{(11)}=-1$, $Z_{21}^{(11)}=-1$ and $Z_{22}^{(11)}=1$ are the elements of one of 4 vectors, for example.

The relation is Eq. 9 is expressed as follows, by using the above quantities:

$$\sum_{j=1}^{(3-1)(3-1)} A_{i,j}Z_j^{(k)} = \lambda_{k_1k_2}Z_i^{(k)}.$$

For example:

$$A_{1,1}Z_1^{(k_1,k_2)}+A_{1,2}Z_2^{(k_1,k_2)}+A_{1,3}Z_3^{(k_1,k_2)}+A_{1,4}Z_4^{(k_1,k_2)} = \lambda_{k_1,k_2}Z_1^{(k_1k_2)},$$

where

$$k_1 = 0, 1 \text{ and } k_2 = 0, 1.$$

Eigenenergy ε_k is given according to the Hückel method as follows.[21,27]

$$\varepsilon_k = \alpha + \lambda_k\beta, \quad (12)$$

where α and β are the Coulomb integral and the resonance integral respectively of orbitals concerned with adsorbed hydrogen atoms. (See Eqs. 2, 3, 4, 5, and 6.). An integral β is taken to be negative (attractive) in accordance with our recent study.[26]

The number of energy levels calculated from Eq. 12 per energy width $\Delta\varepsilon$ is defined as the density of states (D.O.S.). The way of dependence of D.O.S. on eigenenergies, i.e., the distribution of D.O.S. is then obtained. A voltammogram can be estimated from the above distribution. In this procedure a secular equation has, for example, 10000 dimensions for $M\times N=100\times 100$ lattice points. However the expression reduces to a simple one because of an ideal arrangement of the lattice points at single crystal surfaces.

The calculation contains only three parameters: a Coulomb integral α, resonance integral β, and an overlap integral S if necessary.

2.3. Assignment of α, β, and S. Empirical data for negative end potential l, peak potential p, and positive end potential r of the respective hydrogen waves are listed in Table 1 (See also Refs. 28, 29, and 30).

The overlap integral S was taken to be zero as a first approximation since the interactions between adsorbed hydrogen atoms are not expected to be large.

(i) The Relatation of Eigenenergy ε_k and the Potentials. The values of α and β were determined semiempirically by using the potentials at the negative end potential of the hydrogen wave (l) and at the peak (p). It must be mentioned that the electrochemical system and the macromolecule treated in the present calculation have different energy references. Therefore, a parameter (denoted d) is inevitably required to compensate the difference at the comparison of the theoretical and experimental results. (See also Section 4-2 for a discussion about d.)

The eigenenergies are expressed as follows:

$$\varepsilon_k = p + d. \tag{13}$$

$$\varepsilon_k = l + d. \tag{14}$$

$$\varepsilon_k = r + d. \tag{15}$$

or generally

$$\varepsilon_k = \text{potential} + d, \tag{16}$$

where d is a parameter to be discussed later.

(ii) Assignment on the Respective Planes.

Pt(111). There are $M \times N$ eigenenergies ε_k's among which $\alpha+6\beta$, $\alpha-2\beta$, and $\alpha-3\beta$ are the lowest energy, the energy corresponding to the peak and the highest energy, where β is taken negative, as stated earlier. The energies $\alpha+6\beta$ and $\alpha-2\beta$ correspond to the negative end potential l and the peak potential p of the butterfly on Pt(111), respectively. Thus we have

$$\alpha - 2\beta - d = p \text{ (0.79 V vs. RHE from Table 1)}$$
$$\alpha + 6\beta - d = l \text{ (0.54 V vs. RHE from Table 1)}$$

The above two relations give the following expressions for α and β:

$$\alpha = -2\beta + d + (p+l)/2 = d + 0.73 \text{ (eV vs. RHE)} \tag{17}$$

$$\beta = (l-p)/8 = -0.031 \text{ (eV vs. RHE)} \tag{18}$$

Pt(100). Similarly, α and $\alpha+4\beta$ correspond to the peak potential p and a negative end potential l of the hydrogen wave, respectively.

$$\alpha - d = p \text{ (0.35 V vs. RHE from Table 1)} \tag{19}$$

$$\alpha + 4\beta - d = l \text{ (0.05 V vs. RHE from Table 1)} \tag{20}$$

The above two relations give the following expressions for α and β:

$$\alpha = d + 0.35 \text{ (eV vs. RHE).} \tag{21}$$

$$\beta = (l-p)/4 = -0.075 \text{ (eV vs. RHE).} \tag{22}$$

Pt(110). The same relations of Eqs. 19 and 20 hold for Pt(110). However, the values of α and β expressed by one-election Hamiltonians depend indirectly on distances. Two unit distances R and $\sqrt{2}R$ between a hydrogen atom of interest and the nearest neighbours will give two sets of values α_1, β_1, and α_2, β_2, respectively.

The negative end value l is common for both cases of R and $\sqrt{2}R$:

$$\alpha_1 + 4\beta_1 - d = \alpha_2 + 4\beta_2 - d = l.$$

The above equation leads to the following expression:

$$(\alpha_1 + \alpha_2)/2 + 2(\beta_1 + \beta_2) - d = l.$$

Displacements of $(\alpha_1+\alpha_2)/2$ with α and of $\beta_1+\beta_2$ with $(1+\rho)\beta$ where ρ is a parameter to be adjusted below, yields:

$$\alpha + 2(1+\rho)\beta - d = l \text{ (0.05 V vs. RHE from Table 1)} \tag{23}$$

D.O.S.–eigenvalue graph reveals two peaks and reproduces the peak potentials (Table 1, $p_1=\alpha_1=0.14$ eV, $p_2=\alpha_2=0.22$ eV vs. RHE) at $\rho=0.6$. Thus we obtain:

$$\alpha = d + 0.18 \text{ (eV vs. RHE)} \tag{24}$$

$$\beta = (l-p)/2(1+\rho) = -0.041 \text{ (eV vs. RHE)} \tag{25}$$

The final values of α and β are listed in Table 2. These values are discussed later.

2.4. Calculated Results. Figure 3 shows a typical D.O.S.–eigenvalue graph obtained on Pt(111) lattice with $M \times N = 200 \times 200$. The eigenvalue for the peak is -33 (arbitrary units) which corresponds to the eigenenergy $\alpha-2\beta$. Empirically observed butterfly is compared in Fig. 1 by adjusting the total number of energy levels to that of adsorbed hydrogen atoms. The total number of the adsorbed hydrogen atoms was estimated by subtracting the minimum current due to charging up the double layer. The abscissas of voltammogram and D.O.S.–eigenenergy graph have an unit of V and eV, respectively. Symbols ↓ in Fig. 1 indicate the potentials used for determining the values of α and β.

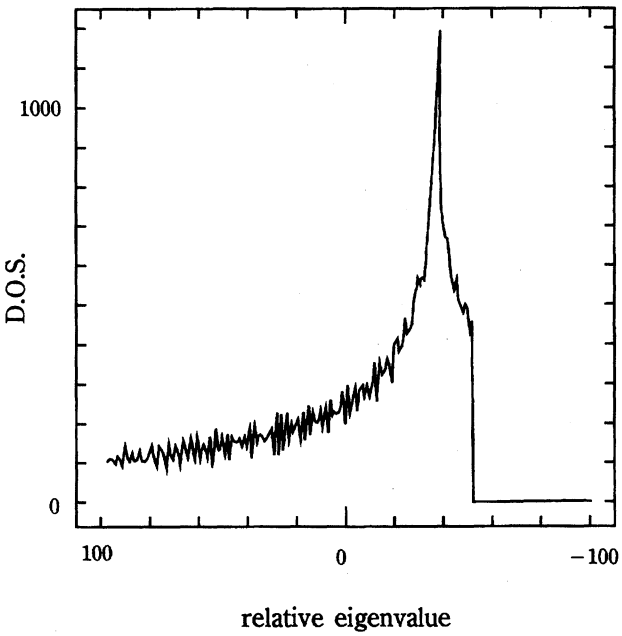

Fig. 3. D.O.S. vs. relative eigenvalues on the lattice Pt(111), $M \times N = 200 \times 200$.

Table 2. Coulomb and Resonance Integrals

Lattices	α		β	
	Expressions	Values	Expressions	Values
(111)	$\alpha=-2\beta+d+p+l$	$0.73+d$/eV	$\beta=(l-p)/8$	−0.031 eV
(100)	$\alpha=-4\beta+d+l$	$0.35+d$/eV	$\beta=(l-p)/4$	−0.075 eV
(110)	$\alpha=-2(1+\rho)\beta+d+l$	$0.18+d$/eV	$\beta=(l-p)/2(1+\rho)$	−0.041 eV

Calculated results represented by a smooth solid line (M=400 and N=200) gives definitely the peak at the specified position with a rapid decay at the positive side. It must be also noted that the calculated curve ends up at 0.82 V, in agreement with the experimental wave.

Thus, the present analysis will be taken as succeeding in reproducing essential aspects of the experimental results. However, the butterfly shows a hump at the negative side of the peak which is not reproduced by the calculation. This will be discussed later (Section 4).

Results on the other planes are shown in Fig. 2, where solid and dotted lines represent the calculated (M=400 and N=200) and experimental (0.1 M $HClO_4$) results. The original graph with small vibrations as shown in Fig. 3 is also smoothed in Fig. 2. Symbols ↓ indicate the potentials used for determining the values of α, β, and ρ.

The calculated result on Pt(100), Fig. 2a, gives a symmetrical peak and covers the potential range of the hydrogen wave satisfactorily. The symmetrical nature is due to the lack of the 3rd term of Eq. 10 in Eq. 11. The graph with small vibrations as shown in Fig. 3 is also smoothed.

On Pt(110), the calculated result (M=400 and N=200) also reproduces two peaks as shown in Fig. 2b, though both peak heights are the same, in contrast to the observed results.

Effect of the size of the domain is discussed in Section 4.

The resonance integral β represents the interaction among adsorbed hydrogen atoms. Their values were estimated from the negative end potential and the peak potential as $-1.2RT$ mol^{-1} (0.031 eV), $-2.9RT$ mol^{-1} (0.075 eV) and $-1.6RT$ mol^{-1} (0.041 eV) for Pt(111), Pt(100), and Pt(110), respectively (Table 2). We have previously analyzed the hydrogen wave on Pt(110) by using an adsorption isotherm derived kinetically under the presence of the interaction among adsorbates.[26] The estimated interaction appeared attractive and its energy was $-1.8RT$ mol^{-1}. The present value of $-1.6RT$ mol^{-1} for Pt(110) coincides satisfactorily with the previous value.

In the statistic-mechanical analysis,[14,16] the repulsive interaction was assumed on the basis of the model that the adsorbed hydrogen atom forms a localized bond with surface metal atom and that the localized bonds do not resonate. Only the remaining interaction between the bonds was taken as repulsive. The present treatment, however, confirms the attractive interaction.

It will be stressed that the hydrogen waves can be explained by the relatively simple analysis of the Hückel method with the attractive interaction.

3. Analysis of the Square Wave on Pt(111) Lattice

3.1. Model of Delocalized Adsorbates and Its D.O.S. It is assumed in the following analysis that the hydrogen atoms or their electrons (simply denoted particles for the time being) move freely in a 2-dimensional adsorbed layer like free electrons of a metal. Consider a square adsorption layer of length a for simplicity. Momenta of a particle moving in the adsorbed layer are given by two quantum numbers n_x and n_y, where x and y are coordinates of the layer. The energy ε_n of a particle with quantum numbers n_x and n_y is given as

$$\varepsilon_n = h^2(n_x^2+n_y^2)/8ma^2 \tag{26}$$

where m and h have the usual meanings. The number of energy levels having energies less than ε_n, is estimated by drawing a circle of radius R on 2-dimensional quantum number space, where R is given as follows:

$$R^2 = n_x^2+n_y^2 = 8ma^2\varepsilon_n/h^2 \tag{27}$$

The number of representative points within the circle, i.e., the number of energy levels of interest, ν, is given as:[21]

$$\nu = \pi R^2/4 = \pi(n_x^2+n_y^2)/4. \tag{28}$$

The factor 1/4 originates from conditions $n_x \geqq 0$ and $n_y \geqq 0$. Equations 26 and 28 give the following expression for ν.

$$\nu = (2\pi ma^2/h^2)\cdot\varepsilon_n. \tag{29}$$

The number of energy levels appears to be proportional to energy ε_n. D.O.S. is directly obtained by differentiating the above equation with ε_n:

$$\text{D.O.S.} = \mathrm{d}\nu/\mathrm{d}\varepsilon_n = 2\pi ma^2/h^2 = \text{const.} \tag{30}$$

D.O.S. appears constant, independent of ε_n, when particles are assumed to move freely.

The square wave is characterized by a constant current of the ionization of the adsorbed hydrogen (the backward reaction of Eq. 1):

$$\mathrm{H(a)} \rightarrow \mathrm{H^+ + e^-} \tag{31}$$

in the potential range of 0.05—0.35 V. Namely, the number of the hydrogen atoms to be ionized is independent of the potential, i.e., the adsorption energy. This is in agreement with the conclusion of Eq. 30 derived from the free particle model.

3.2. Decision of the Kind of Free Particle. This treatment is further examined by clarifying whether the free

particle is a hydrogen atom or an electron. The charge of the square wave, Q, is estimated by integrating the square wave current i, as 2/3 of the monolayer charge. Namely,

$$Q = \int_0^t i\mathrm{d}t = \int_{v_1}^{v_2} i\cdot \mathrm{d}V/v = 160\ (\mu\mathrm{C\,cm^{-2}}), \tag{32}$$

where v expresses a sweeping rate;

$$v \equiv \mathrm{d}V/\mathrm{d}t\ (\mathrm{V\,s^{-1}}).$$

The number of hydrogen atoms N is given from Q as

$$N = Q\ (\mathrm{C\,cm^{-2}})N_\mathrm{A}\ (\mathrm{mol^{-1}})/F\ (\mathrm{C\,mol^{-1}}) \tag{33}$$

where N_A and F have the usual meanings. N is also estimated from Eq. 30 for unit area as follows.

$$N = \int_{0.05}^{0.4} (\mathrm{d}\nu/\mathrm{d}\varepsilon)\mathrm{d}\varepsilon = (2\pi m/h^2)(eV_2 - eV_1) \tag{34}$$

where V_2 and V_1 are the potentials of both ends of the square wave. The value of m obtained from the above two equations can decide which particle of hydrogen atom and its electron concerns the phenomena. The number N calculated from Eq. 33, 9.98×10^{14} ($\mathrm{cm^{-2}}$) and the value of V_2-V_1 (0.35 eV) give $m=12.4\times10^{-30}$ (kg) from Eq. 34. This value is very close to the rest mass of an electron $m_\mathrm{e}=0.91\times10^{-30}$ (kg) and very far from the rest mass of a proton, $m_\mathrm{p}=1700\times10^{-30}$ (kg). The value of m is ca. 1/140 of the mass of proton. Therefore the particle cannot be a proton. This supports strongly the assertion that the particles moving freely in the 2-dimensional adsorption layer are electrons. Up to the present time the adsorbed hydrogen atoms have been taken to be immobile species because of the chemical bonds with surface metal atoms. The above conclusion is entirely different. Since each energy level accommodates two electrons, a more plausible value of the mass will be a half of the above, i.e., $m=6.2\times10^{-30}$ (kg). This value is ca. 6 times of the rest mass of an electron. This difference will be attributed to several factors such as the over-simplified model, the surface imperfections and rearrangement of a single crystal and so on. Whether each proton remains localized on each adsorption site or becomes delocalized is not decided at present. This is an interesting subject to be solved.

Other hydrogen atoms of the butterfly on Pt(111) and of the hydrogen waves on Pt(100) and Pt(110) are localized at adsorption sites.

This section concludes that when the coverage of the adsorbed hydrogen exceeds ca. 2/3, on Pt(111), the adsorbed hydrogen dissociates to $\mathrm{H_{ad}^+}$ and $\mathrm{e_{ad}^-}$ and the electron $\mathrm{e_{ad}^-}$ moves freely in the adsorption layer, forming its own energy band at the surface. The energy band will be pinned and $\mathrm{e_{ad}^-}$ will be transfered to the conduction band when the electrode potential becomes more positive and $\mathrm{H_{ad}^+}$ will be released into the solution. The resulting ionization current forms the square wave due to the band structure of $\mathrm{e_{ad}^-}$.

4. Discussions

To be discussed are 1) the effect of M and N on D.O.S.–eigenvalue graphs, in order to show the appropriateness of the value of M and N used in the text, 2) the parameter d introduced for adjusting the energy reference of the D.O.S.–eigenvalue graphs to that of voltammograms, and 3) a tentative expansion of the 2-dimensional lattice model to the 3-dimensional one in order to explain the hump of the 'butterfly' in Fig. 1.

One thing to be added before the discussion is the possibility that the 'butterfly' on Pt(111) is related to a formation of adsorbed OH from $\mathrm{OH^-}$.[22] Even if this is the case, the present treatment will not be essentially affected if the requirement of a single electron transfer is satisfied.

4-1. Effect of M and N on D.O.S.–Eigenvalue Graphs. The effect of the elementary domain size on D.O.S.–eigenvalue graphs was examined by varying $M\times N$ from 2×2 to 400×400. A typical D.O.S.–eigenvalue graph at $M\times N=50\times50$ was examined. The essential features were the same as those of Fig. 3 ($M = 200$, $N = 200$) but the periodic fluctuations appeared much stronger. The number of the levels was 2500 and was not sufficient to describe the D.O.S.–eigenvalue graph properly. With the increase of M and N, the fluctuations decreased considerably and a difference at $M = N = 200$ and $M = 400$, $N = 200$ became very small. Thus, the calculations on the other planes were conducted at $M = 400$ and $N = 200$.

A stripe-like domain with the condition of $M(N)\gg N(M)$ by keeping the product $M\times N$ constant (2500), gave even larger fluctuations than those of the case mentioned above ($M = N = 50$). Thus the stripe-like domain was discarded. The vibrations will be attributed to the cosine functions included in Eqs. 10 and 11.

4-2. Parameter d. Eigenenergies ε_k obtained from the Hückel approximation represent the value of the macromolecule in vacuum. On the other hand, the voltammogram is measured in electrochemical system and the potential is referred to the reversible hydrogen electrode. The difference in the energy references should be taken into account.

In the previous study,[3] the Coulomb integrals α appeared positive, though the Coulomb integral is generally negative in the Hückel theory.[27] These 'apparent Coulomb integrals' are taken to contain an additional negative term d due to the difference of the energy reference for the electrochemical system.

The parameter does not appear in the expression of β's, as shown in Eqs. 18, 22, and 25. This means that the integrals β's are directly determined without ambiguity from experimental voltammograms.

Since the electrode potential represents the energy of electron at the Fermi level of the electrode metal referred to that of the standard hydrogen electrode, its value referred to the energy level in vacuum will be obtained by adding the so-called 'absolute' potential of the standard hydrogen electrode.[31,32] Therefore the parameter d directly relates to the 'absolute' potential.

Provided that the value $-d$ is equal to the absolute potential of the standard hydrogen electrode of 4.5 eV,[31,32] the Coulomb integrals $0.73+d$, $0.35+d$, and $0.18+d$ on Pt(111), Pt(100), and Pt(110) turn out negative, as expected from the

usual Coulomb integrals.[27]

4-3. 3-Dimensional Lattices. As mentioned in the analysis of the butterfly on Pt(111), a sharp peak was explained by the Hückel method but a hump observed in the negative side (Fig. 1) of the peak could not be reproduced. It will be of interest to see the effect of the expansion of the present treatment to a 3-dimensional adsorption layer.

The expansion means that we assume the hydrogen absorption into platinum. However, Pt is not a good hydrogen absorbent and the thickness of the layer will be limited to rather thin values.

The theoretical treatments for the 3-dimensional lattices with edges have been reported, to examine the nature of the surface.[34,35] Since the present study is limited to only qualitative aspects of the effect, the 3-dimensional lattice without edges, i.e., the lattice with boundary conditions is treated so that the eigenvalue problem can be analytically solved. Each lattice point is now described by 3 coordinates (i_1, i_2, i_3).

The 3-dimensional interactions have the following matrix elements for Pt(111):

$$\begin{aligned} A_{i,j,j} = {} & \delta(i_1,j_1+1)\times\delta(i_2,j_2)\times\delta(i_3,j_3) \\ & +\delta(i_1,j_1+1)\times\delta(i_2,j_2+1)\times\delta(i_3,j_3) \\ & +\delta(i_1,j_1)\times\delta(i_2,j_2+1)\times\delta(i_3,j_3) \\ & +\delta(i_1,j_1-1)\times\delta(i_2,j_2)\times\delta(i_3,j_3) \\ & +\delta(i_1,j_1-1)\times\delta(i_2,j_2-1)\times\delta(i_3,j_3) \\ & +\delta(i_1,j_1)\times\delta(i_2,j_2-1)\times\delta(i_3,j_3) \\ & +\delta(i_1,j_1)\times\delta(i_2,j_2)\times\delta(i_3,j_3+1) \\ & +\delta(i_1,j_1)\times\delta(i_2,j_2)\times\delta(i_3,j_3-1). \end{aligned} \tag{35}$$

The corresponding equations for Pt(100) and Pt(110) are obtained by deleting the 2nd and 5th terms from the above equation. By using the following Fourier-type eigenvector $Z_j^{(k)}$,

$$Z_j^{(k)} \equiv e_1(k_1j_1)e_2(k_2j_2)e_3(k_3j_3), \tag{36}$$

where $e_1(k_1j_1)$ etc., are defined as in Eq. 8, the following eigenvalue problem

$$\sum_j A_{ijj}Z_j^{(k)} = \sum_{j_1j_2j_3} A_{ijj}e_1(k_1j_1)e_2(k_2j_2)e_3(k_3j_3). \tag{37}$$

was solved. The upper limits of Σ were $(M-1)$, $(N-1)$, and $(L-1)$, where L is the number of the lattice point in the 3rd direction. The final expressions for the eigenvalues for Pt(111), Pt(100), and Pt(110) are given as follows:

Pt(111).

$$\begin{aligned} \lambda_{k_1k_2k_3} = {} & 2\{\cos 2\pi k_1/M + \cos 2\pi k_2/N + \cos 2\pi k_3/L \\ & +\cos(2\pi k_1/M + 2\pi k_2/N)\} \end{aligned} \tag{38}$$

Pt(100) and Pt(110).

$$\lambda_{k_1k_2k_3} = 2(\cos 2\pi k_1/M + \cos 2m\pi k_2/N + \cos 2\pi k_3/L). \tag{39}$$

The results on Pt(111) with L=3 show that a new D.O.S. curve of small size superimposes on the curve similar to that of the 2-dimensional lattice (Fig. 3). The new curve has also a very similar shape to the 2-dimensional one, but with a narrower width with respect to the relative eigenvalue. The results offer many aspects which must be further examined in detail, before we reach a proper reasoning for each of them. However, to be noted is that the new curve locates to the left side of the main peak as the hump does in the voltammogram. In the calculation, we assume the presence of hydrogen atoms with a ratio of one to one for H to Pt in the second and third layers. When the ratio of hydrogen atom is reduced, the new curve will be weakened. Thus the present results may be taken to indicate a positive effect of the hydrogen absorption.

The calculation with $L = 2$ gave essentially the same results. At $L \geqq 4$, the D.O.S. curve became rather complicated and is beyond our interest since the hydrogen does not dissolve so much.

Figure 4 shows the D.O.S.–eigenvalue graph of $3(L)\times200(M)\times200(N)$ for Pt(100). Here again the hydrogen absorption affects D.O.S. and reveals another peak of a similar size to the left side of the main peak in D.O.S.–eigenvalue graph. In fact, the hydrogen wave for Pt(100) reveals two peaks as stated earlier, especially in H_2SO_4 solution. The calculations at $L = 2$ and $L \geqq 4$ gave the results discussed above for Pt(111).

It will be required in the next stage to examine the treatment of the 3-dimensional lattice based on more refined, realistic models.

5. Conclusion

Hydrogen waves on Pt(111), Pt(100), and Pt(110), except the square wave part on Pt(111), were qualitatively explained by the Hückel method applied to an elementary domain with periodic boundary conditions. The equations for the eigen-

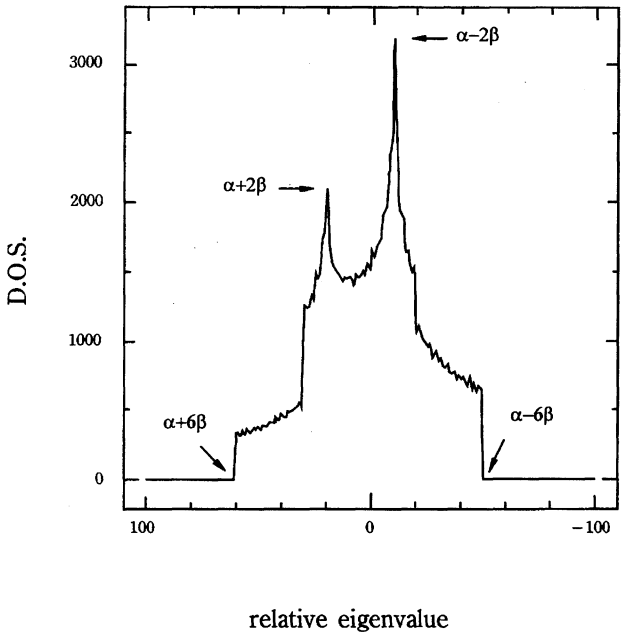

Fig. 4. D.O.S. vs. relative eigenvalues on a 3-dimensional lattice. $L\times M\times N=3\times200\times200$.

values were derived by expressing matrix elements by δ functions. D.O.S. (density of states) – eigenvalue relation allowed us to simulate the voltammograms.

The simulated results on Pt(111) reproduced the observed sharp spike and the rapidly decaying current after the spike on the positive-going scan.

The results on Pt(100) gave almost a symmetrical peak with tails on both side which covered the experimental wave satisfactorily.

The hydrogen wave with two peaks on Pt(110) was reproduced by introducing a parameter due to the unsymmetry of the lattice.

The resonance integral β, was -1.2, -2.9, and $-1.6RT$ mol^{-1} for Pt(111), Pt(100), and Pt(110), showing that the interaction among adsorbed hydrogen atoms is attractive in all cases. The value of Pt(110) coincided with the interaction energy estimated by using the adsorption isotherm derived kinetically. The coincidence demonstrates the validity of the present treatment.

The square wave part on Pt(111) was explained by an entirely new model of a freely moving particle. The constant current density between 0.05 and 0.35 V on Pt(111) was reproduced from D.O.S. distribution calculated based on the model.

The kind of the freely moving particle was decided to be an electron from the calculated mass of 6.2×10^{-30} (kg) which is close to the rest mass of an electron 0.9×10^{-30} (kg) and far from that of a proton, 1700×10^{-30} (kg).

The size effect of the elementary domain was examined. The least number of lattice points required was concluded to ca. M=200 and N=200 arranged in a square shape.

The three dimensional lattice of the adsorbed hydrogen atoms was discussed in order to examine the hump observed in the negative side of the butterfly on Pt(111). The number of layers was limited since Pt is a poor hydrogen absorber. The D.O.S.–eigenvalue graph with two and three layers revealed another peak at the left side of the main peak. This demonstrates a strong effect of the hydrogen absorption. Similar results was obtained on Pt (100).

The author is grateful to Emeritus Professor Hideaki Kita, Associate Professor Akiko Aramata of Hokkaido University and Professor Haruo Hosoya of Ochanomizu University for their discussions and encouragement. He thanks Dr. Hiroshi Murakami of Tokyo Metropolitan College for his advice in the calculations.

References

1) J. Clavilier, R. Faure, G. Guinet, and R. Durand, *J. Electroanal. Chem.*, **107**, 205 (1980).
2) H. Kita and K. Shimazu, *Hyomen*, **26**, 561 (1988).
3) H. Narumi, H. Kita, and H. Murakami, *Chem. Lett.*, **1995**, 35.
4) H. Narumi and H. Kita, "Intn'l Chem. Cong. Pacific Basin. Soc.," Hawaii, Dec. 1995, Abstr., Phys. Chem., No. 753.
5) H. Narumi and H. Hosoya, *Bull. Chem. Soc. Jpn.*, **53**, 1228 (1980).
6) H. Narumi and H. Hosoya, *Bull. Chem. Soc. Jpn.*, **58**, 1778 (1985).
7) H. Narumi, *MATCH*, **22**, 195 (1987).
8) H. Narumi and H. Hosoya, *J. Math. Chem.*, **3**, 383 (1989).
9) H. Narumi, H. Hosoya, and H. Murakami, *J. Math. Phys.*, **32**, 1885 (1991).
10) H. Narumi and H. Hosoya, *J. Math. Phys.*, **34**, 1043 (1993).
11) H. Narumi, H. Kita, and H. Hosoya, *J. Math. Chem.*, **16**, 221 (1994).
12) H. Narumi and H. Kita, *MATCH*, **30**, 225 (1994).
13) H. Narumi, H. Kita, and H. Hosoya, *J. Math. Chem.*, **20**, 67 (1996).
14) J. Horiuti and H. Kita, *J. Res. Inst. Catalysis, Hokkaido Univ.*, **12**, 122 (1964).
15) J. O'M. Bockris and S. Srinivasan, *J. Electrochem. Soc.*, **111**, 858 (1964).
16) H. Kita, *J. Res. Inst. Catalysis, Hokkaido Univ.*, **17**, 77 (1969).
17) H. Matsuda, K. Aoki, and K. Tokuda, *J. Electroanal. Chem.*, **217**, 1 (1987).
18) H. Matsuda, K. Aoki, and K. Tokuda, *J. Electroanal. Chem.*, **217**, 15 (1987).
19) A. Ishihara, "Statistical Physics," Academic Press, Inc., New York (1971), Chap. 8, Sect. 4.
20) H. E. Stanley, "Introduction to Phase Transition and Critical Phenomena," Clarendon Press, Oxford (1971), Appendix B.
21) P.A.Cox, "The Electronic Structure and Chemistry of Solids," Oxford University Press, New York (1987), Chap. 4.
22) K. Al. J. Golze, D. M. Kolb, and D. Scherson, *J. Electroanal. Chem.*, **200**, 353 (1986).
23) S. Ye, H. Kita, and A. Aramata, *J. Electroanal. Chem.*, **333**, 299 (1992).
24) J. Clavilier and D. Armand, *J. Electroanal. Chem.*, **199**, 187 (1986).
25) N. Nishihara, I. A. Raspini, H. Kondoh, H. Shindo, M. Kaise, and H. Nozoye, *J. Electroanal. Chem.*, **338**, 299 (1992).
26) H. Kita, H. Narumi, S. Ye, and H. Naohara, *J. Appl. Electrochem.*, **23**, 589 (1993).
27) E. Heilbronner and H. Bock, "Das HMO-Modell und Seine Anwendung," Verlag Chemie, Gmbh., (1970).
28) A. Rodes, M. A. Zamakhchari, K. El Achi, and J. Clavilier, *J. Electroanal. Chem.*, **305**, 115 (1991).
29) A. Rodes, J. Clavilier, J. M. Orts, T. M. Feliu, and A. Aldaz, *J. Electroanal. Chem.*, **338**, 317 (1992).
30) R. Goméz and J. Clavilier, *J. Electroanal. Chem.*, **354**, 189 (1993).
31) S. Trasatti, *J. Electroanal. Chem.*, **139**, 1 (1982).
32) S. Trasatti, *Electrochim. Acta*, **36**, 1659 (1991).
33) M. P. Sumino and S. Shibata, *Electrochim. Acta*, **37**, 2629 (1992).
34) A. Zangwill, "Physics at Surface," Cambridge University Press, Cambridge (1988), Chap. 4, Sect. 4.
35) R. Hoffmann, "Solid and Surfaces," VCH Publishers, Inc., (1988), Chap. 24.